

Flexible PET/EVA-Based Piezoelectret Generator for Energy Harvesting in Harsh Environments

Zhong, Junwen; Zhong, Qize; Zang, Xining; Wu, Nan; Li, Wenbo; Chu, Yao; Lin, Liwei

2017

Zhong, J., Zhong, Q., Zang, X., Wu, N., Li, W., Chu, Y., et al. (2017). Flexible PET/EVA-Based Piezoelectret Generator for Energy Harvesting in Harsh Environments. *Nano Energy*, 37, 268-274.

<https://hdl.handle.net/10356/83115>

<https://doi.org/10.1016/j.nanoen.2017.05.034>

© 2017 Elsevier. This is the author created version of a work that has been peer reviewed and accepted for publication by *Nano Energy*, Elsevier. It incorporates referee's comments but changes resulting from the publishing process, such as copyediting, structural formatting, may not be reflected in this document. The published version is available at: [<http://dx.doi.org/10.1016/j.nanoen.2017.05.034>].

Downloaded on 13 Jul 2024 21:17:16 SGT

Flexible PET/EVA-Based Piezoelectret Generator for Energy

Harvesting in Harsh Environments

Junwen Zhong,^a Qize Zhong,^b Xining Zang,^a Nan Wu,^c Wenbo Li,^c Yao Chu,^{a, d} and Liwei Lin^{a, d*}

^aDepartment of Mechanical Engineering, University of California at Berkeley, Berkeley, California, 94720, United States

^bTemasek Laboratories (TL@ NTU), Nanyang Technological University, 50 Nanyang Drive, 637553, Singapore

^cWuhan National Laboratory for Optoelectronics, and School of Optical and Electronic Information, Huazhong University of Science and Technology, Wuhan, 430074, China.

^dSensors and Microsystems Laboratory, Tsinghua-Berkeley Shenzhen Institute, Shenzhen, 518055, China

J. W. Zhong and Q. Z. Zhong contributed equally to this work.

* Corresponding author.

E-mail: lwlin@me.berkeley.edu

Abstract Stable and repeatable operation is paramount for practical and extensive applications of all energy harvesters. Herein, we develop a new type of flexible piezoelectret generator, which converts mechanical energy into electricity consistently even under harsh environments. Specifically, the generator, with piezoelectric coefficient (d_{33}) reaching ~ 6300 pC/N, had worked stably for continuous ~ 90000 cycles, and the generator pressed by a human hand produced load peak current and power up to ~ 29.6 μ A and ~ 0.444 mW, respectively. Moreover, the capability to steadily produce electrical power under extreme moisture and temperature up to 70 °C had been achieved for possible applications in wearable devices and flexible electronics.

Keywords: mechanical energy, flexible generator, harsh environment, piezoelectret

Introduction

With the rise of intelligent wearable electronics, energy harvesters converting ambient mechanical energy into electricity have attracted much attention, which is not only because the energy source (e.g. human body movement, airflow, sound vibration, water waves *etc.*) ubiquitously exists in ambient background and is free, but also because the converting energy could enable these electronics to be functional indefinitely, thereby reducing the dependence on battery power.¹⁻³ Recently, flexible generators based on different working mechanism mainly including piezoelectric,^{4, 5} electromagnetic^{1, 6} and electrostatic effect^{3, 7-17} have been successfully demonstrated with typical applications in mobile health care,^{8, 13} human-machine interaction,^{9, 14} wireless communication¹⁵ and self-charging cells^{10, 11}, *etc.* Among these generators, flexible electrostatic generators like triboelectric generators^{3, 7-12} and electret generators¹³⁻¹⁷, have obtained more interests due to their simple fabrication process, high conversion efficiency and environmentally friendly without chemical processing. However, the output properties and stability of those generators are mainly determined by the surface surplus charges,^{15, 18, 19} which will be neutralized, once exposed to the moist air atmosphere, impairing the output performance of generators.²⁰⁻²² Thus, well encapsulation of these electrostatic generators is required to endure long-term exposure to harsh environments. Previously, Guo *et al.* demonstrated a water-proof triboelectric generator that could be driven by the water flow,²³ and Lee *et al.* had developed a fully packaged triboelectric sensors array for mapping the distribution of foot produced pressure.²⁴ However, the additional packaging material would add volume and reduce the flexibility of the generators.^{15, 20} New strategy with minimum packaging materials and low impact on the flexibility should be considered for flexible generators operating under harsh environments.

Flexible piezoelectret, known of high piezoelectric coefficient (d_{33}), light-weight and low-cost, *etc.*, has extensive transducer applications, such as energy harvesters²⁵⁻²⁸ and loudspeakers²⁹. Since the electric dipole-like charges are produced inside the materials,²⁵ the piezoelectret generators, one kind of electrostatic generators, have the potential to be excellent energy harvester candidates that still can perform well in harsh environments. In this work, we present a new type of flexible piezoelectret generator based on the polyethylene terephthalate

(PET) electret film and the ethylene vinyl acetate copolymer (EVA) adhesive layer *via* a hot-pressing method. The corona charging technique was used to generate megascopic electric dipoles inside a big air bubble of the generator. Mechanical push and release the generator will change the dipole moments of the electric dipoles and alter the electrostatic induction intensity to generate alternating electricity, with d_{33} coefficient reaching ~ 6300 pC/N and stable outputs for continuous ~ 90000 operations. Experimentally, the generator pressed by a human hand produced load peak current and power up to ~ 29.6 μ A and ~ 0.444 mW, respectively. Moreover, the most prominent advantage of this generator is the remarkable output stability under harsh environments of extreme moisture and temperature up to 70 °C, indicating that the generator may be suitable for wearable energy harvesting and used in other harsh environments.

Results and Discussion

Fabrication of the flexible PET/EVA-based piezoelectret generator

The detailed fabrication steps of the flexible PET/EVA-based piezoelectret generator are schematically given in **Figure 1a** and **Figure S1**. The raw material was the flexible ~ 45 μ m-thick PET electret film with the ~ 25 μ m-thick and ring-shape EVA adhesive layer at the boundary, which was defined as the EVA/PET laminated film (**Figure 1b**). The cross-section view scanning electron microscope (SEM) image (**Figure 1c**) clearly shows the EVA/PET laminated structure. The surface morphology of the PET electret film was investigated by atomic force microscope (AFM), indicating the PET surface roughness varied from ~ -82 to ~ 78 nm (**Figure S2**). In theory, the rough surface morphology is helpful to capture more surplus charges. The charges capturing ability of the PET electret film was studied *via* the corona charging method,¹⁵ as indicated in **Figure S3**. In this work, two PET electret films were charged with positive and negative high voltages (values of 20 and -20 kV), respectively, and then the corresponding surface potential *versus* time curves were measured (**Figure 1d**). It's found that the surface potential for positive and negative charging still maintained at about 0.52 and -0.50 kV after 50 days, respectively. These results indicate that the PET electret film is an excellent electret material, with the ability to capture and maintain both positive and negative surplus charges for a long time.

The fabrication steps began with fixing four polydimethylsiloxane (PDMS) spacers (size

of $0.5 \times 0.25 \text{ cm}^2$, thickness of 1 mm) on four corners of the EVA/PET laminated film (**Figure S1-I and Figure S4a**). Subsequently, another EVA/PET laminated film placed at the top was bonded to the laminated film with spacers *via* a hot-pressing method (**Figure 1-I, Figure S1-II**), forming the PET/EVA/PET laminated film with an arch-shaped air bubble with the height of 0.5-1 mm (**Figure S4b**). The cross-section view SEM image indicates that the two EVA/PET laminated films were bonded tightly (**Figure 1e**). Moreover, the PET/EVA/PET laminated film could stand the shearing force up to $\sim 33 \text{ N/cm}^2$ before separation, indicating the strong mechanical bonding characteristics (**Figure 1f**).

The as-fabricated PET/EVA/PET laminated film was then corona charged, in order to generate megascopic electric dipoles inside the air bubble (**Figure S1-III**).²⁶ In the next step, aluminum (Al) adhesive tape (thickness of $\sim 100 \text{ }\mu\text{m}$) was covered on two outside surfaces of the charged PET/EVA/PET laminated film, as the electrodes (**Figure S1-IV**). Lastly, two protective layers (water proof tape, thickness of $\sim 50 \text{ }\mu\text{m}$) were covered on two Al electrodes (**Figure S1-V**), forming a PET/EVA-based flexible electret generator with effective area of about $\sim 4 \times 4 \text{ cm}^2$ (**Figure 1-II and Figure 1g**).

Working mechanism of the PET/EVA-based flexible piezoelectret generator

By virtue of the megascopic electric dipoles inside the air bubbles, piezoelectret materials have the piezoelectric-like property as the traditional piezoelectric materials, similar to lead zirconate titanate (PZT), zinc oxide (ZnO) and polyvinylidene fluoride (PVDF), *etc.*^{25, 30, 31} Herein, the corona charging method was used to generate electric dipoles inside the air bubble of the PET/EVA/PET laminated film before the two electrodes were added on the outer surfaces, as shown in **Figure 2a**. Specifically, high voltage up to -20 kV was applied on the corona needle for about 3 min, with samples placed about 5 cm below the needle tip. Under the strong electric field intensity, the air in the air bubble was broken down to generate ionic charges with both polarities. The positive and negative ionic charges were driven by the electric field, and captured by the upper and lower inner PET surfaces, respectively. As a result, the air bubble with charged PET inner surfaces worked as megascopic electric dipoles.

The short circuit thermally stimulated discharge (TSD) method was employed to verify the existence of electric dipoles (**Figure S5**). Specifically, our laminated film and PET raw film

were corona charged first, and then two outer surfaces were covered by Al electrodes. The samples were heated in a thermal chamber with a temperature rising rate of 3 °C/min, and the induced current curves were recorded in-situ by an electrometer. If there are electric dipoles, measurable electrical current peak in the heating process can be measured. As indicated in **Figure 2b**, the measured current curve of the PET/EVA/PET laminated film consisted of a current peak started at about 70 °C and ended at about 110 °C, with the maximum peak value located at about 90 °C. The influences from the potential shape changes of the air bubble were negligible as no visible output currents were measured before 70 °C. In comparison, no significant current peak was observed in the short circuit TSD current curve of the PET raw electret film.

To measure the quasi-static piezoelectric d_{33} coefficient, a generator was operated by a give force F and the corresponding short-circuit output current was recorded (**Figure S6a**). The value of transferred charges Q was achieved by integrating the current over time (**Figure S6b**), and the d_{33} coefficient can be calculated:²⁶

$$d_{33} = Q/F \quad (1)$$

The d_{33} coefficient of our generator reached ~ 6300 pC/N, which was significantly larger than that of generators based on traditional cellular polypropylene (PP) piezoelectret film (**Figure 2c**).^{26, 32} This outstanding piezoelectric property is attributed to the excellent charges capturing ability of PET electret and low elastic modulus of the air bubble structure. Moreover, the stability of d_{33} coefficient was investigated by placing the generator in indoor atmosphere for weeks and it maintained in a narrow range around the original value for 6 weeks, as indicated in **Figure 2c**.

Based on above piezoelectric-like behavior, **Figure 2d** schematically illustrates the power generating processes of the generator. At any states, the megascopic electric dipoles will generate induced charges on the top and bottom Al electrodes, and the charge density on the electrode (σ_e) is decided by the following equation:²⁷

$$\sigma_e = -\varepsilon_0 \varepsilon E = \frac{\varepsilon \sigma_0}{\left(\frac{D_1}{D_2} + \varepsilon\right)} \quad (2)$$

where ε_0 and ε are the dielectric constant of air and relative dielectric constant of PET,

respectively. E is the electric field in the PET layer and σ_0 represents the charge density captured by the PET inner surface. D_1 is the thickness of PET layer and D_2 is thickness of air bubble or the dipole moments of the megascopic electric dipoles. In our case, ϵ_0 , ϵ , E , σ_0 , and D_1 are constants, and σ_e is affected by D_2 .

Figures 2d-f show a non-sinusoidal excitation (hand pressing motion) of the generator with the resulting open-circuit voltage response and short-circuit current response. In the original state (**Figure 2d-I**), the electrical potential between the two electrodes are in equilibrium state, and no open-circuit voltage or short-circuit current can be observed (**Figure 2e-I and Figure 2f-I**). When the generator is compressed (**Figure 2d-I to III**, during the very short **state II**), D_2 decreases and the charge densities on the top and bottom electrodes also decrease. The open circuit voltage curve increases in the whole compressing process (**Figure 2e-I to III**). The short circuit current curve increases to positive peak value (**Fig. 2f-I to II**) and then drops to zero (**Fig. 2f-II to III**), resulting a sharp positive current peak. As the compression state maintains (**Figure 2d-III**), a new equilibrium is established. The open-circuit voltage keeps at the highest value (**Figure 2e-III**) and the short circuit current keeps at zero (**Figure 2f-III**). It is noted that most of the surplus charges will not be neutralized when the two PET layers are contacted with each other, which is benefit by the rough surface morphology of the PET (**Figure S2**). If the generator is released (**Figure 2d-III to I**, during the very short state II), D_2 increases because of the mechanical elasticity of the generator. The charge density on both electrodes will increase. The open-circuit voltage drops from highest value to zero (**Fig. 2e III to I**). The short circuit current increases to negative peak value (**Fig. 2f-III to IV**) and then drops to zero (**Fig. 2f-IV to I**), resulting a sharp negative current peak. At last, the electrical potential between the two electrodes become in equilibrium state again.

In general, the basic working mechanism of the generator is the electrostatic induction effect caused by the megascopic electric dipoles. Compressing and releasing the generator will change the dipole moments of the electric dipoles. Thus, the electrical potential between the two electrodes are changed, and the alternating electricity is generated. Switching polarity tests were also carried out to confirm that the measured output signals are generated from the generator rather than from the artifacts of the measurement system (given in the right side of

Figure 2e and Figure 2f).

Electrical output properties of the flexible PET/EVA-based piezoelectret generator

The electrical outputs of the flexible PET/EVA-based piezoelectret generator were carefully investigated by periodically compressing and releasing at controlled pressure and frequency. Typically, the generator was attached to a force meter, which was tightly fixed onto an x-y-z mechanical stage.

By virtue of the large piezoelectric d_{33} coefficient, the output properties of our generator were excellent. Under given applied pressure of 6.67 kPa and sinusoidal frequency of 5 Hz, the load peak current and power density of the generator with different external resistors were measured (**Figure 3a**). The maximum load peak power density reached $\sim 25.923 \mu\text{W}/\text{cm}^2$, when the corresponding load peak current density and load resistance were $\sim 0.241 \mu\text{A}/\text{cm}^2$ and $60 \text{ M}\Omega$, respectively. It should be noted that unless otherwise specified, the load resistance is $60 \text{ M}\Omega$ for optimal outputs for the prototype system.

The load peak current density and corresponding transferred charge density ($\Delta\sigma$) for the generator under given applied frequency of 5 Hz and different applied pressure is given in **Figure 3b**. It's found that when the applied pressure was less than 1.33 kPa, the load peak current density increased approximately linearly. As the applied pressure increased to be higher than 1.33 kPa, the load peak current density increased approximately linearly too, with a smaller increasing rate. The variation tendency of the $\Delta\sigma$ was similar to that of the load peak current density, which was divided to two regions. These output behaviors are similar to the "vertical contact-separation mode triboelectric generator".³³ The load peak current density and $\Delta\sigma$ reached $\sim 0.239 \mu\text{A}/\text{cm}^2$ and $\sim 6.648 \text{ nC}/\text{cm}^2$, respectively, when the applied pressure reached 6.67 kPa. By continuously increasing the applied pressure, the peak current and corresponding transferred charge density of our generator tended to be saturated, as the air bubble was completely compressed.

Furthermore, the load peak current density and $\Delta\sigma$ increased step by step under given applied pressure of 6.67 kPa and different applied frequency, from $\sim 0.077 \mu\text{A}/\text{cm}^2$ at 1.2 Hz to $\sim 0.237 \mu\text{A}/\text{cm}^2$ at 5 Hz. However, the $\Delta\sigma$ almost kept at a constant value of $\sim 6.650 \text{ nC}/\text{cm}^2$ for different applied frequency (**Figure 3c**). According to the above results, the load peak

current density of the generator is related to both of the applied pressure and frequency, and the $\Delta\sigma$ is only related to applied pressure.

The output stability performance of the generator was studied by pressing and releasing for continuous ~ 90000 cycles, under given applied pressure and frequency of 6.67 kPa and 5 Hz, respectively. As indicated in **Figure 3d**, both of the load peak current density and $\Delta\sigma$ remained at the constant values of $\sim 0.245 \mu\text{A}/\text{cm}^2$ and $\sim 6.645 \text{nC}/\text{cm}^2$. This remarkable stability performance is attribute to the excellent charges capturing ability of PET electret and good flexibility and elasticity of the generator.

Stability of the flexible PET/EVA-based piezoelectret generator under harsh environments

As the megascopic electric dipoles exist inside the flexible PET/EVA-based piezoelectret generator and the electrodes are well protected, this generator has the great potential in harvesting mechanical energy under harsh environments. The stability of the generator under extreme moisture environment was investigated. Specifically, the generator was placed into a closed space full of water vapor and continuously operated under given applied pressure and frequency of 6.67 kPa and 5 Hz, respectively (**Figure S7**). Typical load current curves generated by the generator in one second were recorded for every 5 min (**Figure 4a**). The load peak current density varied between $\sim 0.256 \mu\text{A}/\text{cm}^2$ and $\sim 0.268 \mu\text{A}/\text{cm}^2$ for the whole 25 min of measurement. Moreover, the generator was soaked into water (**Figure 4b**), and 6 blue LEDs connected in series were lit up by hand pressing the generator (**Figure 4c and Video 1**). The turn-on threshold voltage of the 6 blue LEDs was $\sim 15 \text{V}$ (**Figure S8**) and the highest peak current went through the LEDs was $\sim 29.6 \mu\text{A}$ (**Figure 4d**). Therefore, the generator generated an instantaneous output power of $\sim 0.444 \text{mW}$. Above results indicated that our generator had the outstanding ability in converting the mechanical energy into electricity under the extreme moisture environment or even completely immersed in water.

In comparison, an arch-shaped flexible generator (**insert in Figure 4e**) based on PET electret film was also operated under the high water vapor environment. In this case, the surplus charges contacted with extreme moisture directly. The load peak current density dropped from $\sim 0.197 \mu\text{A}/\text{cm}^2$ to $\sim 0.0185 \mu\text{A}/\text{cm}^2$ after continuously operating for 10 min. Then, the generator was only operated for 3 seconds at each 5 min time interval after removing the vapor, the output current of the generator could not recover again (**Figure 4e**).

The output performance of the flexible PET/EVA-based piezoelectret generator under

different temperatures was characterized. A heater was used to control the temperature of the generator, which was continuously operated under the applied pressure and frequency of 6.67 kPa and 5 Hz (**Figure S9**). As given in **Figure 4f**, when the temperatures increased from 30 °C to 70 °C, the load peak current density only had relatively stable outputs between $\sim 0.251 \mu\text{A}/\text{cm}^2$ and $\sim 0.263 \mu\text{A}/\text{cm}^2$. If the temperature was then kept at 70 °C for 25 min, the output currents remained stable. However, higher temperature can cause the loss of the megascopic electric dipoles inside the generator based on the short circuit TSD measurement result (**Figure 2b**). As such, the output performance of the generator would reduce (**Figure S10**).

Conclusions

In summary, a new type of flexible piezoelectret generator based on EVA/PET laminated film was fabricated, in which megascopic electric dipoles were captured inside the air bubble. By changing the dipole moments of the electric dipoles, the generator converted mechanical energy into electricity effectively, with d_{33} coefficient reaching $\sim 6300 \text{ pC}/\text{N}$. Specifically, load peak current and corresponding peak power of $\sim 29.6 \mu\text{A}$ and $\sim 0.444 \text{ mW}$ were reached by hand pressing the generator, and stable outputs were achieved for ~ 90000 continuous working cycles. More importantly, the generator had remarkable output stability under harsh environments with extreme moisture and temperature up to 70 °C, indicating the feasibility for wearable energy harvesting. This study provides a new, simple and efficient strategy for designing robust and reliable flexible energy harvesting devices.

Acknowledgements

This work was financially supported by the National Natural Science Foundation of China (51322210, 61434001, 51372132). Professor Liwei Lin is a core-principal investigator of Tsinghua-Berkeley Shenzhen Institute (TBSI) and we acknowledge the funding support of TBSI. The authors would like to thank facility support of the center for Nanoscale Characterization & Devices (CNCD), WNLO-HUST and the Analysis and Testing Center of Huazhong University of Science and Technology.

Appendix A. Supplementary materials

Supplementary data associated with this article can be found in the online version at.....

References

- [1] A. D. Kuo, *Science* 309 (2005) 1686.
- [2] C. Chang, V. H. Tran, J. Wang, Y. -K. Fuh, L. Lin, *Nano Lett.* 10 (2010) 726.
- [3] F. -R. Fan, Z. -Q. Tian, Z. L. Wang, *Nano Energy* 1 (2012) 328.
- [4] L. Persano, C. Dagdeviren, Y. Su, Y. Zhang, S. Girardo, D. Pisignano, Y. Huang, J. A. Rogers, *Nat. Commun.* 4 (2013) 1633.
- [5] Y. Qi, M. C. McAlpine, *Energy Environ. Sci.* 3 (2010) 1275.
- [6] J. M. Donelan, Q. Li, V. Naing, J. A. Hoffer, D. J. Weber, A. D. Kuo, *Science* 319 (2008) 807.
- [7] Z. L. Wang, J. Chen, L. Lin, *Energy Environ. Sci.* 8 (2015) 2250.
- [8] J. Yang, J. Chen, Y. Su, Q. Jing, Z. Li, F. Yi, X. Wen, Z. Wang, Z. L. Wang, *Adv. Mater.* 27. (2015) 1316.
- [9] B. -U. Hwang, J. -H. Lee, T. Q. Trung, E. Roh, D. -I. Kim, S. -W. Kim, N. -E. Lee, *ACS Nano* 9 (2015) 8801.
- [10] A. Ramadoss, B. Saravanakumar, S. W. Lee, Y. -S. Kim, S. J. Kim, Z. L. Wang, *ACS Nano* 9 (2015) 4337.
- [11] H. Guo, M. -H. Yeh, Y. -C. Lai, Y. Zi, C. Wu, Z. Wen, C. Hu, Z. L. Wang, *ACS Nano* 10 (2016) 10580.
- [12] H. Kang, H. Kim, S. Kim, H. J. Shin, S. Cheon, J. -H. Huh, D. Y. Lee, S. Lee, S. -W. Kim, J. H. Cho, *Adv. Funct. Mater.* 26 (2016) 7717.
- [13] J. Zhong, Y. Zhang, Q. Zhong, Q. Hu, B. Hu, Z. L. Wang, J. Zhou, *ACS Nano* 8 (2014) 6273.
- [14] J. Zhong, H. Zhu, Q. Zhong, J. Dai, W. Li, S. -H. Jang, Y. Yao, D. Henderson, Q. Hu, L. Hu, J. Zhou, *ACS Nano* 9 (2015) 7399.
- [15] J. Zhong, Q. Zhong, G. Chen, B. Hu, S. Zhao, X. Li, N. Wu, W. Li, H. Yu, J. Zhou, *Energy Environ. Sci.* 9 (2016) 3085.
- [16] Y. S. Ko, F. A. Nüesch, D. Damjanovic, D. M. Opris, *Adv. Mater.* 29 (2016) 1603813.
- [17] T. Vu-Cong, C. Jean-Mistral, A. Sylvestre, *Smart Mater. Struct.* 22 (2013) 025012.

- [18] G. M. Sessler, *J. Electrostat.* 51 (2001) 137.
- [19] J. Zhong, Q. Zhong, F. Fan, Y. Zhang, S. Wang, B. Hu, Z. L. Wang, J. Zhou, *Nano Energy* 2 (2013) 491.
- [20] Y. Yang, H. Zhang, R. Liu, X. Wen, T. -C. Hou, Z. L. Wang, *Adv. Energy Mater.* 3 (2013) 1563.
- [21] L. Gu, N. Cui, J. Liu, Y. Zheng, S. Bai, Y. Qin, *Nanoscale* 7 (2015) 18049.
- [22] V. Nguyen, R. Yang, *Nano Energy* 2 (2013) 604.
- [23] H. Guo, Z. Wen, Y. Zi, M. -H. Yeh, J. Wang, L. Zhu, C. Hu, Z. L. Wang, *Adv. Energy Mater.* 6. (2016) 1501593.
- [24] K. Y. Lee, H. -J. Yoon, T. Jiang, X. Wen, W. Seung, S. -W. Kim, Z. L. Wang, *Adv. Energy Mater.* 6 (2016) 1502566.
- [25] S. Bauer, R. Gerhard-Multhaupt, G. M. Sessler, *Phys. Today* 57 (2004) 37.
- [26] N. Wu, X. Cheng, Q. Zhong, J. Zhong, W. Li, B. Wang, B. Hu, J. Zhou, *Adv. Funct. Mater.* 25 (2015) 4788.
- [27] W. Li, N. Wu, J. Zhong, Q. Zhong, S. Zhao, B. Wang, X. Cheng, S. Li, K. Liu, B. Hu, J. Zhou, *Adv. Funct. Mater.* 26 (2016) 1964.
- [28] B. Wang, C. Liu, Y. Xiao, J. Zhong, W. Li, Y. Cheng, B. Hu, L. Huang, J. Zhou, *Nano Energy* 32 (2017) 42.
- [29] J. Hillenbrand, G.M. Sessler, *Ferroelectrics* 472 (2014) 77.
- [30] X. Zhang, G.M. Sessler, Y. Wang, *J. Appl. Phys.* 116 (2014) 074109.
- [31] P. Pondrom, J. Hillenbrand, G. M. Sessler, J. Bös, T. Melz, *Appl. Phys. Lett.* 104 (2014) 172901.
- [32] Q. Zhong, J. Zhong, X. Cheng, X. Yao, B. Wang, W. Li, N. Wu, K. Liu, B. Hu, J. Zhou, *Adv. Mater.* 27 (2015) 7130.
- [33] L. Lin, Y. Xie, S. Wang, W. Wu, S. Niu, X. Wen, Z.L. Wang, *ACS Nano* 7 (2013) 8266.

Figures

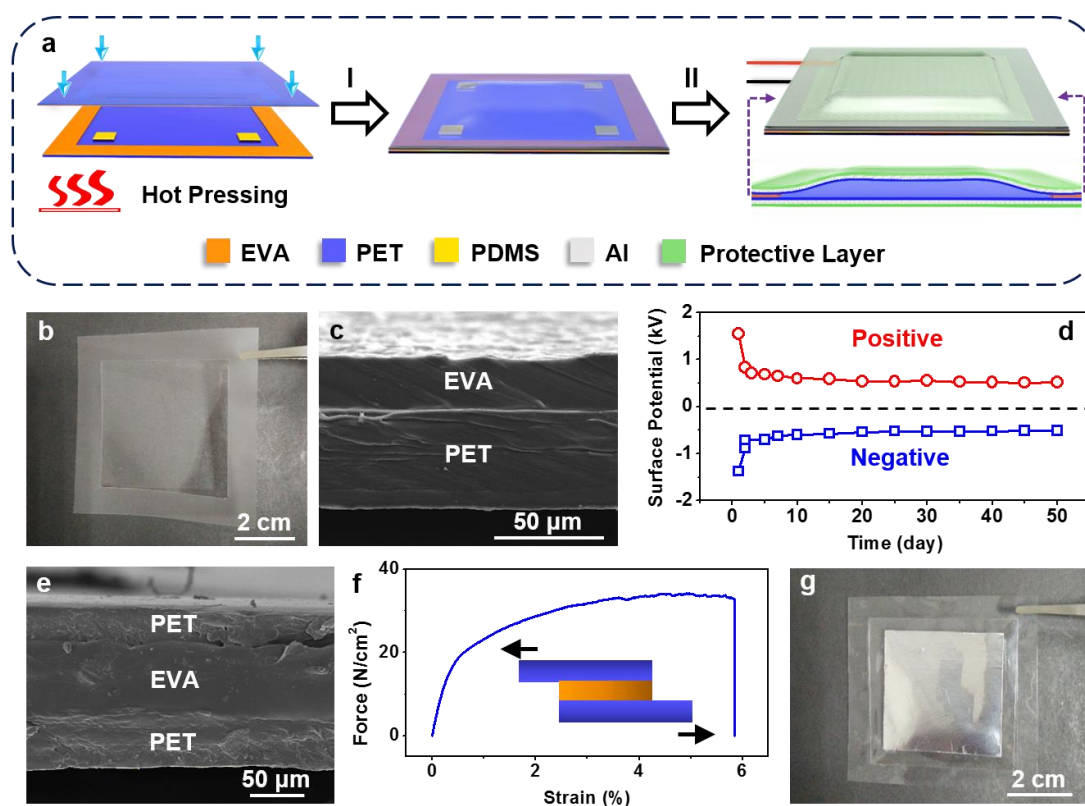


Figure 1. Fabrication of the flexible PET/EVA-based piezoelectret generator. (a) Schematic diagram showing the fabrication steps of the generator, (I) hot pressing and corona charging; (II) placing and adhesion of the electrodes and protective layers. (b) An optical photo of the EVA/PET laminated film. (c) Cross-section view SEM image of the EVA/PET laminated film. (d) Surface potential *versus* time curves for the PET electret with positive and negative corona charging, showing little decay after the first 5 days. (e) Cross-section view SEM image of the PET/EVA/PET laminated film. (f) Mechanical shear testing result of the PET/EVA/PET laminated film. (g) An optical photo showing a fabricated generator.

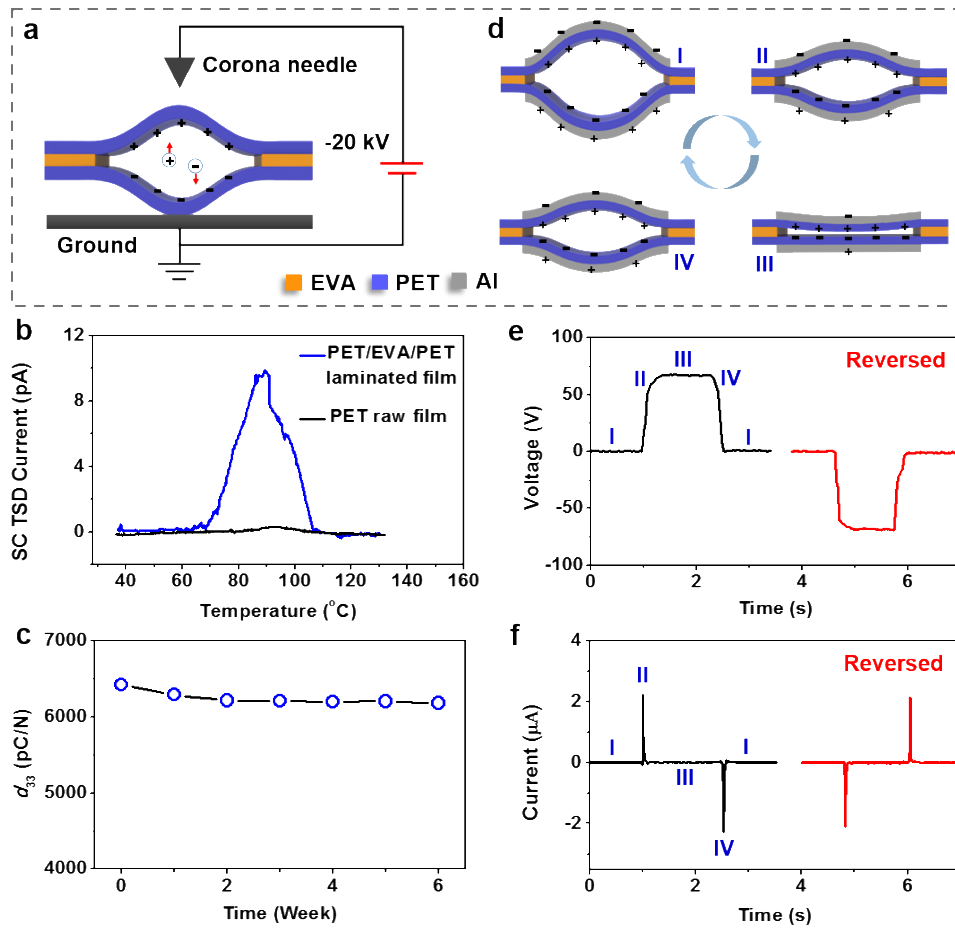


Figure 2. Working mechanism of the flexible PET/EVA-based piezoelectret generator. (a) Schematic diagram indicating the corona charging method. (b) Short circuit TSD current measurement results for the PET/EVA/PET laminated film and PET raw film. (c) The characterized d_{33} coefficient for the generator placed in the indoor atmosphere for 6 weeks. (d) Schematic diagram indicating the electricity generation of the generator when it is at (I) original, (II) compressing, (III) equilibrium and (IV) releasing states, respectively. (e) Open-circuit voltages and (f) short-circuit currents for the generator when it was forward-connected and reverse-connected to the measurement system, respectively.

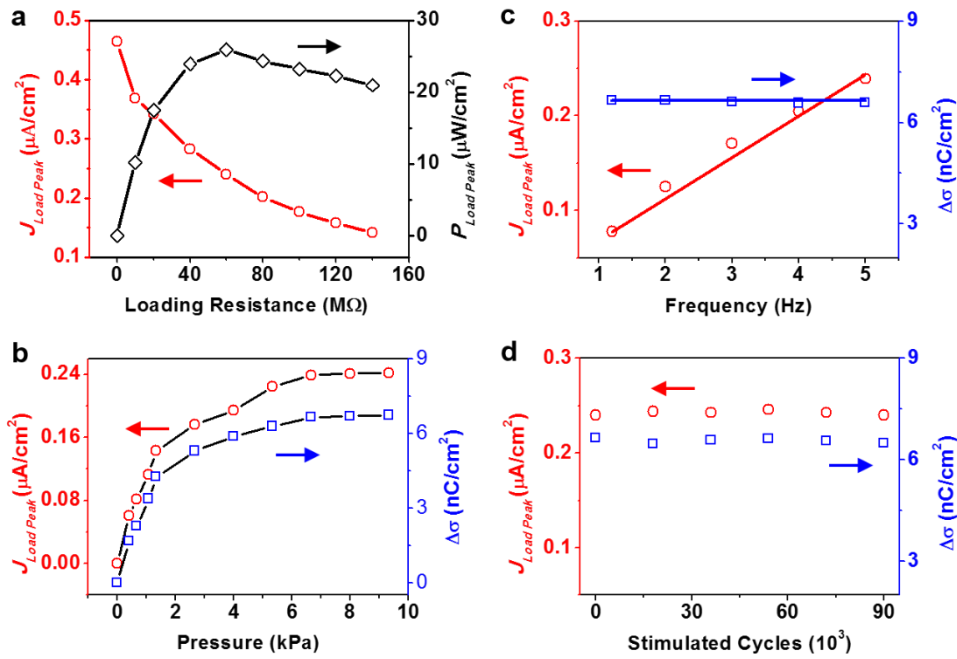


Figure 3. Electrical outputs of the flexible PET/EVA-based piezoelectret generator. (a) Load peak current and power density of a generator with respect to different load resistances, Under given applied pressure of 6.67 kPa and sinusoidal frequency of 5 Hz. (b) Load peak current and transferred charge density for a generator with respect to given applied frequency of 5 Hz and different applied pressure. (c) Load peak current and transferred charge density for a generator respect to given applied pressure of 6.67 kPa and different applied frequency. (d) Load peak current and transferred charge density for a generator for continuous operations of 90000 cycles, under given applied pressure and frequency of 6.67 kPa and 5 Hz.

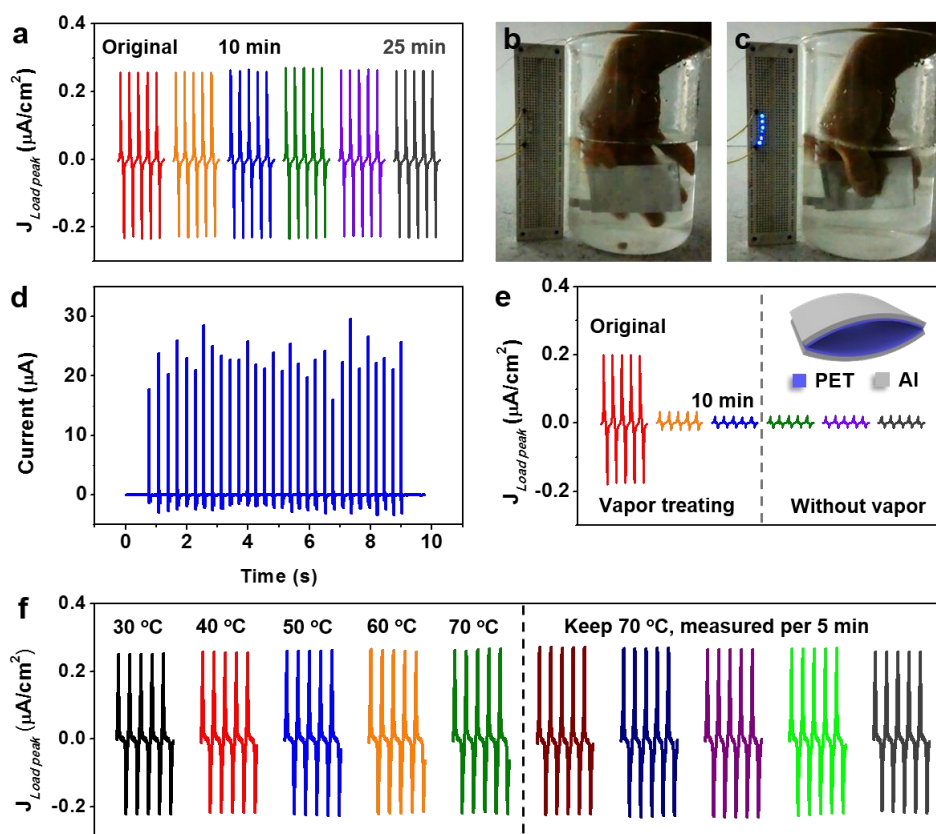


Figure 4. Output stability characterizations of the flexible PET/EVA-based piezoelectret generator under harsh environments. (a) Current outputs of the generator under the high water vapor environment, under given applied pressure of 6.67 kPa and sinusoidal frequency of 5 Hz. Optical photos for (b) the generator under water and (c) 6 blue LEDs lit up by hand pressing the generator under water. (d) Current flowing through the LEDs when they were lit up. (e) Currents outputs for an arch-shaped generator under the high water vapor environment and the following without vapor environment, under given applied pressure and frequency of 6.67 kPa and 5 Hz. Insert in (e) showing the schematic diagram of the arch-shaped generator. (f) Current outputs for a flexible PET/EVA-based piezoelectret generator when the temperature increased from 30 °C to 70 °C and then kept at 70 °C, under given applied pressure and frequency of 6.67 kPa and 5 Hz.